Nanomed. J., 3(4): 248-252, Autumn 2016

ORIGINAL RESEARCH PAPER

Effects of ultrasound on properties of ni-metal organic framework nanostructures

Abbas Pardakhty [1]; Mehdi Ranjbar [2]*

[1]*Pharmaceutics Research Center, Institute of Neuropharmacology, Kerman University of Medical Sciences, Kerman, Iran*

[2]*Department of Chemistry, Kerman Branch, Islamic Azad University, Kerman, Iran*

ABSTRACT

Objective(s): According to the unique properties of magnetic nanoparticles, Nickel Metal-Organic Frameworks (MOF) were synthesized successfully by ultrasound irradiation. Metal-organic frameworks (MOFs), are organic–inorganic hybrid extended networks that are constructed via covalent linkages between metal ions/metal clusters and organic ligands called a linker.

Materials and Methods: The nanoparticles were synthesized by Ultrasound Method Under a synthesis conditions, All chemicals were used as received without further purification. Scanning electron microscopy (SEM) images were obtained on LEO- 1455VP equipped with an energy dispersive X-ray spectroscopy at university of Kashan in Iran. Transition electron microscopy (TEM) images were obtained on EM208 Philips transmission electron microscope with an accelerating voltage of 200 kV.

Results: Results showed that Ni-MOF synthesized by this method, had smaller particle size distribution and It was found that the different kinds of ligand leads to preparation products with different morphologies and textural properties. Moreover, ultrasound irradiation method has significant effect on microstructures of as-synthesized MOFs and can improve their textural properties compared to method without using hydrothermal route.The XRD patterns of the samples obtained from ultrasound irradiation was well matched with that of as-prepared Ni-MOF by solvothermal method.

Conclusion: This rapid method of ultrasonic radiation as compared to the classical solvothermal synthesis, showed promising results in terms of size distribution, surface area, pore diameter and pore volume.

Keywords: *Drug carriers, Ni-MOF, Surface area, Ultrasound irradiation*

How to cite this article

Pardakhty A, Ranjbar M. Effects of Ultrasound on Properties of Ni-Metal Organic Framework Nanostructures. Nanomed J., 2016; 3(4): 248-252.DOI:10.22038/nmj.2016.7582

INTRODUCTION

Recent advances in nanostructured materials have been led by the development of new synthetic methods that provide control over size, morphology, and nano/microstructure [1]. As a new class of microporous/mesoporous materials, metal-organic frameworks (MOFs) are currently investigated as potential candidates for gas storage and separation [2–5]. MOFs exhibit unique shape and size dependent properties such as more accessible active sites within the porous nanocrystals, the ability to functionalize the surfaces of MOF nanocrystals. Also they possess tailorable molecular cavities, adjustable functionality and extremely larger surface area. They have been shown to have potential applications in gas storage and separation [6], catalysis [7], and CO_2 capture [8]. Because it usually consists of two parts, linker (organic ligand) and node (metal cluster), types of MOFs having different textural structures can be easily generated by the simple combination change of these two parts. With the help of above synthesis of MOF, specific pore size and structure based on the

*Corresponding Author Email: *Mehdi.Ranjbar@outlook.com*
Tel: 09366592379

Note. This manuscript was submitted on July 28, 2016; approved on September 31, 2016

molecular level design was obtainable and it characterized MOF as a very novel material compared to zeolites. Thus it has been widely investigated for the application purposes[9-11].

A group of these structural compounds with open metal ions, such as Ni-MOF are found with many promising applications [12]. Ni-MOF is a versatile metal oxide having numerous applications in many fields. It has been used as a catalyst and catalyst support for various organic reactions [13-15]. The relative long synthesis time is always a problem for the solvothermal method. In the past few years, several new synthesis techniques including ultrasound [16], surfactant assisted method [17], and microwave assisted method [18, 19] have been applied in the MOFs synthesis process. compared to the conventional microwave method, the ultrasound method has attracted a great attention because it sharply reduces the overall processing time, increases the product yield and improves the quality of the product. In this work, we synthesised the Ni-MOF in order to understand the influence of the ultrasound irradiation on the pore textural properties and crystalline phase.

MATERIALS AND METHODS

Nickel structures were synthesized by ultrasound irradiation. All chemicals, $Ni(NO_3)_2.6H_2O$, (+99%, Merck), 2,6-Pyridinedicarboxylic acid (99%, Aldrich), ethanol (+99.8%, SigmaAldrich), N,N-dimethyl formamide (DMF) (99%, Merk), were of analytical grade.

Synthesis of Ni-MOF Nanostructure

1.43 mmol (0.4 g) of $Ni(NO_3)_2.6H_2O$ and 0.45 mmol (0.36 g) of pyridine 2,6-dicarboxilic acid were dissolved in 20 mL of ethanol. The mixture was continuously stirred for 2 h at room temperature, and then was placed in a Teflon-lined stainless steel autoclave with 55 mL capacity. Then, the mixture was transferred into a teuon reactor with a tight cap and kept at 60 °C for 4 h. Ultrasound irradiations were carried out on a SONICA-2200 EP, (maximum 305 W at 22 kHz) and TecnoGaz, S.p.A, Tecna 6, (maximum 200 W at 22 kHz) spectra. The products were washed twice with fresh DMF. After mixing and dissolving the reactants, the clear solution was transferred into a Teuon reactor and irradiated in the ultrasonic bath for speciuc sonication time at the predetermined temperature.

Nanoparticles characterization

The FT-IR spectroscopy and XRD analysis were performed in Kashan university, SEM image and N_2 adsorption techniques were obtained in Tehran university. The FT-IR was recorded on a Nicolet Fourier Transform IR, Nicolet 100 spectrometer in the range 500–4000 cm^{1-} using the KBr disk technique. The XRD pattern was carried out on a Philips difractometer. Samples for SEM analysis were coated with a thin layer of gold by a sputter coater device, heating rate was 10 K/min during the experiment from room temperature up to 773 K. N_2 adsorption technique with Belsorp mini model was employed to determine pore textural properties including the surface area, micropore volume and pore size distribution at 80 K.

RESULTS AND DISCUSSION

The ultrasonic irradiation method reduced the reaction time for the synthesis of Ni-MOF (Table 1) and affected the crystalline phase (Fig. 3), particle size (Fig. 4), pore diameter, surface area and volume pore (Table 1) [17-19].

The Fourier transform infrared spectrum of the precursor (Fig. 1) exhibits adsorption peaks including the broad adsorption band centered at 3426 cm^{-1} which was attributed to hydroxyl stretching vibrations, the bands at 2851 cm^{-1} and 2961cm^{-1} which were due to the banding stretch of C-H, the peak appearing around of 1645 cm^{-1} confirmed the presence of carboxylate group in the precursor, the peak appearing around 1385 cm^{-1} confirmed the presence of NO_3 as counter ion in the structure, the bands at 1213 cm^{-1} and 1089 cm^{-1} confirmed the presence of NO and ONO [20], the band at 448 cm^{-1} confirmed the presence of C-N bond in the structure and the band at 400 cm^{-1} corresponded to the presence of Ni-O bond [21]. According to data obtained from the FT-IR spectra, the structure of presented in Fig. 2 was proposed for Ni-MOF.

Fig. 3 shows the evolution of XRD patterns of Ni-MOF following ultrasound irradiation times under a given set of the synthesis conditions of 200 W power and 320 K ultrasound bath temperature. Ultrasound irradiation times varied from 10 to 40 min. Although crystals were not fully grown and the solid phase yield was relatively low, Ni-MOF began to crystallize out within 10 minutes. XRD intensity of the 1st peak at two theta of 6.75° increased with synthesis time until 20 min, indicating that structural deterioration

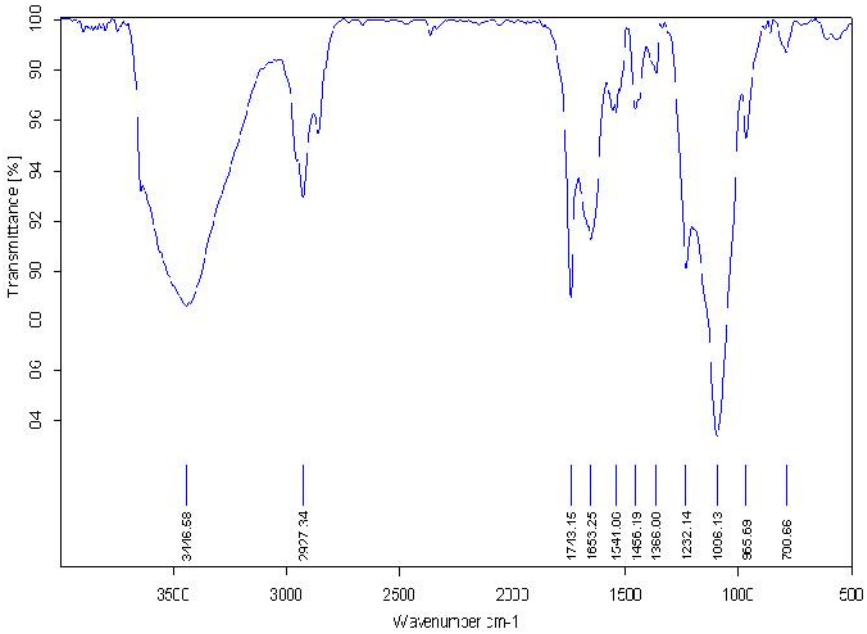

Fig. 1. FT-IR spectra of Ni-MOF produced by ultrasound irradiation

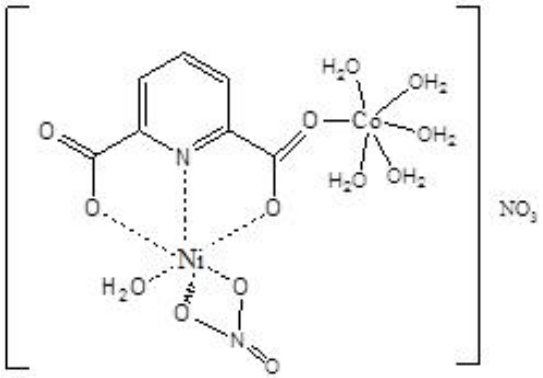

Fig. 2. The structure of Ni-MOF according to spectral data

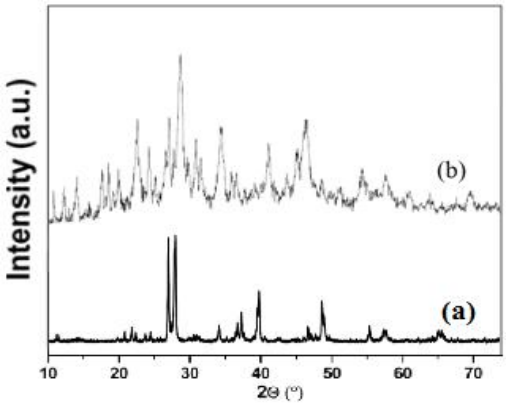

Fig. 3. XRD patterns of Ni-MOF synthesized (a) without ultrasound irradiation, (b) by ultrasound irradiation

of Ni-MOF began after 20 min of irradiation. The XRD patterns of the samples obtained from ultrasound irradiation was well matched with that of as-prepared Ni-MOF by solvothermal method [21].

As shown in Fig 4, it was evodent that the size of crystallin particles and the thickness of Ni-MOF increased with increasing the ultrasound irradiation time. This result was further confirmed by the corresponding XRD patterns (Fig 3). Furthermore, under synthesis conditions, uniform crystals with average size of 3–12 micrometer were produced (Fig. 4) compared to previous reports [22, 23]. Fig 5 illustrates SEM images of samples 3 and 4. The morphology of all samples were particle-like; however, by increasing the reaction temperature, the particle size of the products increased.

The N_2 adsorption technique was used to determine the pore textural properties including the surface area, pore diameter and micropore volume of Ni-MOF (Table 1). Textural properties of the Ni- MOF in this work was different with those reported previously [24] by others in terms of the surface area and pore volume which could be attributed to the effect of ultrasonication on the textural properties of the final product.

Table 1. Effect of ultrasound parametres on on characteristics of Ni- MOF

Samples	Ultrasound Bath temperature (K)	Ultrasound irradiation Time (min)	Frequencies (Hz)	SEM images	N_2 adsorption technique		
					Pore diameter (Å)	Surface area (m2/g)	Pore volume (cm^3/g)
1	20	120	30	A	11.7	950	0.312
2	20	120	30	B	10.1	1030	0.318
3	30	120	30	C	10.4	1530	0.409
4	30	120	30	D	10.3	2230	0.483

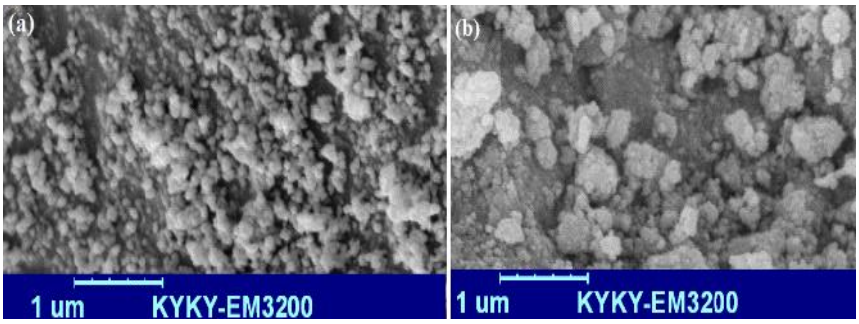

Fig. 4. SEM images of MOF samples a)1 and b) 2. Ultrasound power was supplied at 200 W

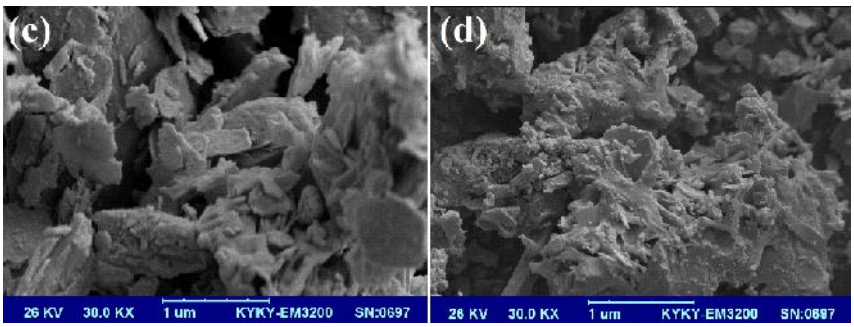

Fig. 5. SEM images of MOF samples c) 3 and d) 4

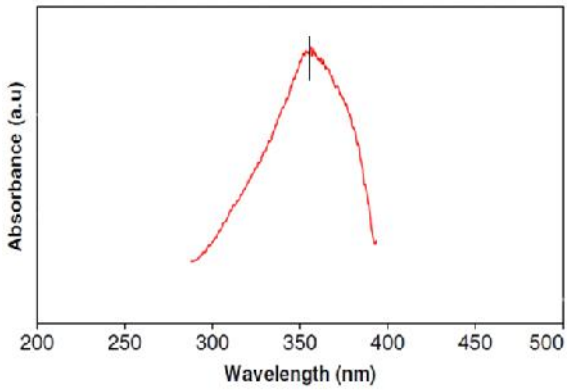

Fig. 6. PL spectra of Ni-MOF nanoparticles at room temperature

The relationship between ultrasound irradiation time and pore textural properties of Ni- MOF was shown in Table 1**.** Based on these results, increase in the ultrasound irradiation time would lead to increase in the surface area, pore diameter, volume pore and particles size. Optical properties of the Ni-MOF nanoparticles at difference reaction conditions investigated by photoluminescence (PL) spectroscopy are given in Fig 6. The spectrum shows the emission peak at 353 nm. The emission spectrum shows a blue shift (1.16 eV), compared to that of the bulk Ni-MOF structures. Such a large blue shift of excitonic absorption band could be attributed to the small crystallite size of the samples [20].

CONCLUSION

In this investigation for first time, hierarchical nanospheres-like Ni-MOFs were successfully synthesized with hydrothermal method. The Ni-MOFs were synthesized at 200 °C for 6–15 h. According to SEM and TEM images, hollow and hierarchical structures for Ni- MOFs were confirmed. This method shows promising results in terms of morphology (surface area about 3000 m^2/g). The ultrasound irradiation time affected on the surface area, particle size, crystalline phase, pore volume and pore diameter. The estimated optical band gap energy is an accepted value for the photocatalytic activities in visible light as well as for application in the drug carriers.

ACKNOWLEDGEMENT

Authors are grateful to council of Kerman University of Medical Sciences, Kerman, Iran.

CONFLICT OF INTEREST

The authors declare that there are no conflicts of interest regarding the publication of this manuscript.

REFERENCES

1. Nehra A, Singh KP. Current trends in nanomaterial embedded field effect transistor-based biosensor. Biosens Bioelectron. 2015; 74 (1): 731-743.
2. Chen KI, Li BR, Chen YT. Silicon nanowire field-effect transistor-based biosensors for biomedical diagnosis and cellular recording investigation. Nano Today. 2011; 30 (2): 131-154.
3. Murray AR, Kisin ER, Tkach AV, Yanamala N, Mercer R, Young SH, Fadeel B, Kagan VE, Shvedova AA. Factoring-in agglomeration of carbon nanotubes and nanofibers for better prediction of their toxicity versus asbestos. Part Fibre Toxicol. 2012; 9(10): 1-19.
4. Pujalté I, Passagne I, Brouillaud B, Tréguer M, Durand E, Ohayon-Courtès C. Cytotoxicity and oxidative stress induced by different metallic nanoparticles on human kidney cells. Part Fibre Toxicol. 2011; 8(10): 1-16.
5. Jeng HA, Swanson J. Toxicity of metal oxide nanoparticles in mammalian cells. J Environ Sci Health. 2006; 41(12): 2699-2711.
6. Song W, Zhang J, Guo J, Zhang J, Ding F, Li L. Role of the dissolved zinc ion and reactive oxygen species in cytotoxicity of ZnO nanoparticles. Toxicol Lett. 2010; 199(3): 389-397.
7. Boonstra J, Post JA. Molecular events associated with reactive oxygen species and cell cycle progression in mammalian cells. Gene. 2004; 33 (7): 1-13.
8. Zabirnyk O, Yezhelyev M, Seleverstov O. Nanoparticles as a novel class of autophagy activators. Autophagy. 2007; 3(3): 278-281.
9. Yu L, Lu Y, Man N, Yu SH, Wen P. Rare earth oxide nanocrystals induce autophagy in HeLa cells. Small. 2009; 5(24): 2784-2787.
10. Chen Y, Yang L, Feng C, Wen P. Nano neodymium oxide induces massive vacuolization and autophagic cell death in non-small cell lung cancer NCI-H460 cells. Biochem Biophys Res. 2005; 337(1): 52-60.
11. Lanone S, Boczkowski J. Biomedical applications and potential health risks of nanomaterials: molecular mechanisms. Curr Mol Med. 2006; 6(6): 651-663.
12. Zhang H, Shan Y, Dong L. A comparison of TiO_2 and ZnO nanoparticles as photosensitizers in photodynamic therapy for cancer. J Biomed Nanotechnol. 2014; 10(8): 1450-1457.
13. Goharshadi EK, Abareshi M, Mehrkhah R, Samiee S, Moosavi M, Youssefi A. Preparation, structural characterization, semiconductor and photoluminescent properties of zinc oxide nanoparticles in a phosphoniumbased ionic liquid. Mat Sci Semicon Proc. 2011; 14(1): 69-72.
14. Goharshadi EK, Ding Y, Jorabchi MN, Nancarrow P. Ultrasound-assisted green synthesis of nanocrystalline ZnO in the ionic liquid [hmim][NTf 2]. Ultrason Sonochem. 2009; 16(1): 120-123.
15. Goharshadi EK, Ding Y, Nancarrow P. Green synthesis of ZnO nanoparticles in a room-temperature ionic liquid 1- ethyl-3-methylimidazolium bis (trifluoromethylsulfonyl) imide. J Phys Chem Solids. 2008; 69(8): 2057-2060.
16. Jalal R, Goharshadi EK, Abareshi M, Moosavi M, Yousefi A, Nancarrow P. ZnO nanofluids: green synthesis, characterization, and antibacterial activity. Mater Chem Phys. 2010; 121(1): 198-201.
17. Moosavi M, Goharshadi EK, Youssefi A. Fabrication, characterization, and measurement of some physico-chemical properties of ZnO nanofluids. Int J Heat Fluid. 2010; 31(4): 599-605.
18. AshaRani P, Low Kah Mun G, Hande MP, Valiyaveettil S. Cytotoxicity and genotoxicity of silver nanoparticles in human cells. ACS Nano. 2008; 3(2): 279-290.
19. Nel A, Xia T, Mädler L, Li N. Toxic potential of materials at the nanolevel. Science. 2006; 311(5761): 622-627.
20. Xia T, Kovochich M, Liong M, Madler L, Gilbert B, Shi H. Comparison of the mechanism of toxicity of zinc oxide and cerium oxide nanoparticles based on dissolution and oxidative stress properties. ACS Nano. 2008; 2(10): 2121-2134.
21. Sharma V, Shukla RK, Saxena N, Parmar D, Das M, Dhawan A. DNA damaging potential of zinc oxide nanoparticles in human epidermal cells. Toxicol Lett. 2009; 185(3): 211-218.
22. Singh N, Manshian B, Jenkins GJ, Griffiths SM, Williams PM, Maffeis TG. NanoGenotoxicology: the DNA damaging potential of engineered nanomaterials. Biomaterials. 2009; 30(23): 3891-3914.
23. Xia T, Kovochich M, Brant J, Hotze M, Sempf J, Oberley T. Comparison of the abilities of ambient and manufactured nanoparticles to induce cellular toxicity according to an oxidative stress paradigm. Nano Lett. 2006; 6(8): 1794-1807.